Detailed Forms of Yield Curves from Semithick Aluminum Targets*

J. G. SKOFRONICK,† J. A. FERRY, D. W. PALMER, G. WENDT‡, AND R. G. HERB
University of Wisconsin, Madison, Wisconsin
(Received 15 April 1964)

Accurate measurements were made of the detailed shapes of γ-ray yield curves from semithick aluminum targets over the 992-keV resonance. Detailed information from these targets was possible through the use of a new electronic device which allowed data to be taken while incrementing the target voltage to provide energy changes and simultaneously correcting for energy fluctuations in the beam. To provide pure targets, fast evaporation rates were used with pressures usually 3×10^{-7} Torr or less. During runs the pressure was usually 3×10^{-9} Torr or less. No contamination effects appeared. Experimental results were compared to curves computed by Monte Carlo techniques for an assumed collision spectrum in which the contributions of electrons from each shell were computed using the Born approximation. These calculated curves gave closer fits to the experimental data than previous curves for which all electrons were assumed to be free and stationary. The experimental results departed somewhat from those calculated because nonuniformities in target thickness were not completely eliminated. Some additional results on thick targets show that surface contamination can take place if O_2 and N_2 gases are introduced into the vacuum system.

I. INTRODUCTION

IN previous published work, the $Al^{27}(p,\gamma)Si^{28}$ resonance reaction at 992 keV has been studied under varying experimental and theoretical conditions.[1–8] Walters *et al.*[1–3] observed that the yield from a high-resolution proton beam incident on a thick target of aluminum exhibited a maximum at an energy slightly above the resonance energy. This maximum had been predicted by Lewis[9] and is a result of the large discrete energy losses suffered by the protons as they pass through the target. They found that the height of the peak (called the Lewis peak) was very dependent upon experimental conditions. To calculate a thick-target yield curve, Walters *et al.*[2,3] assumed all of the electrons of the atom were free, thus the discrete energy-loss probability (henceforth called a collision spectrum) behaved as $1/Q^2$, where Q is the energy lost by the proton. This collision spectrum was used in a computer along with Monte Carlo techniques, to calculate a thick-target yield curve which qualitatively fit experimental data.

Palmer *et al.*[4] extended the Monte Carlo results with the $1/Q^2$ spectrum to both semithick and thick targets. They found that to obtain agreement between calculated curves and experimental data it was necessary to assume very nonuniform targets. In addition they showed that the variation in the height of the Lewis peak could be caused by surface contamination.

Better agreement with experimental thick-target data was obtained by Costello *et al.*,[6,7] who obtained calculated yield curves by the use of a collision spectrum (called C-S spectrum) which was formulated so as to account for the binding effects of the electrons.

Morsell[10,11] tried to gain further knowledge on the collision spectrum by passing a proton beam, with a very narrow energy spread, through thin carbon films where he observed the energy-loss distribution of the protons. By comparing experimental results with results calculated from the $1/Q^2$ spectrum and the C-S spectrum, Morsell was led to reject both of these spectra. He tried a third collision spectrum based on the Born approximation as originally used by Bethe[12] (called B-B spectrum) and found he could obtain satisfactory agreement between calculated and experimental results if nonuniform carbon films were assumed.

Bondelid and Butler[8] have calculated yield curves for semithick and thick targets of aluminum by using the results of Symon[13] even though these results are only qualitatively correct for protons at the energies being considered. By assuming various degrees of oxidation of the target, they were able to get fits to the experimental data.

Prior to the present work, the most dependable data on yield curves from semithick targets was that given by the families of curves presented by Palmer *et al.*[4] It was later shown that the target preparation techniques used in this work were such that contamination effects

* Work supported in part by the U. S. Atomic Energy Commission.
† Present address: Florida State University, Tallahassee, Florida.
‡ Visiting scholar from Finland under the Fubright-Hayes Act.
[1] W. L. Walters, D. G. Costello, J. G. Skofronick, D. W. Palmer, W. E. Kane, and R. G. Herb, Phys. Rev. Letters **7**, 284 (1961).
[2] W. L. Walters, D. G. Costello, J. G. Skofronick, D. W. Palmer, W. E. Kane, and R. G. Herb, Phys. Rev. **125**, 2012 (1962).
[3] W. L. Walters, Ph.D. thesis, University of Wisconsin, 1960 (unpublished); available from Ann Arbor Microfilms Inc., Ann Arbor, Michigan.
[4] D. W. Palmer, J. G. Skofronick, D. G. Costello, A. L. Morsell, W. E. Kane, and R. G. Herb, Phys. Rev. **130**, 1153 (1963).
[5] R. G. Herb, in International Conference on Nuclidic Masses [International Atomic Energy Agency, Vienna, Austria, 1963, (to be published)].
[6] D. G. Costello, Ph.D. thesis, University of Wisconsin, 1963 (unpublished); available from Ann Arbor Microfilms Inc., Ann Arbor, Michigan.
[7] D. G. Costello, J. G. Skofronick, A. L. Morsell, D. W. Palmer, and R. G. Herb, Nucl. Phys. **51**, 113 (1964).
[8] R. O. Bondelid and J. W. Butler, Phys. Rev. **130**, 1078 (1963).
[9] H. W. Lewis, Phys. Rev. **125**, 937 (1962).
[10] A. L. Morsell, Ph.D. thesis, University of Wisconsin, 1963 (unpublished); available from Ann Arbor Microfilms Inc., Ann Arbor, Michigan.
[11] A. L. Morsell, Phys. Rev. **135**, A1436 (1964).
[12] H. A. Bethe, Ann. Physik **5**, 325 (1930).
[13] K. R. Symon, Ph.D. thesis, Harvard University, 1948 (unpublished).

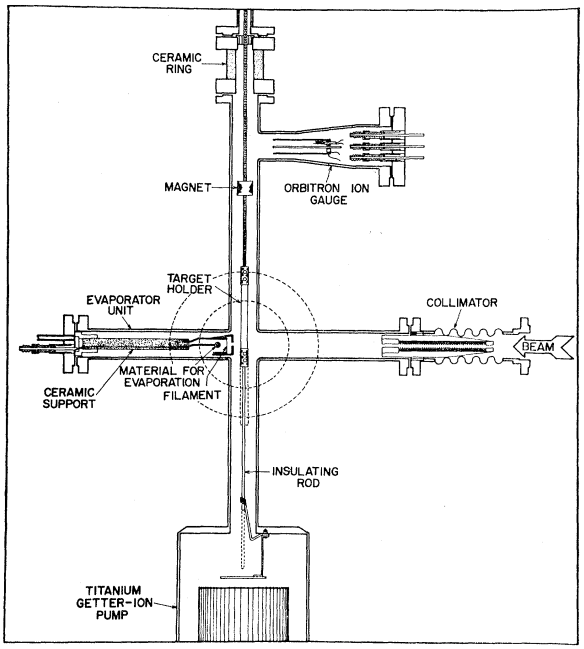

FIG. 1. Target chamber.

were certain to be present. Also, later analysis showed that background contributions had substantial effects on the form of the curves. In addition, the calculated curves used the $1/Q^2$ spectrum which is now known to be inferior.

In this paper, a study of the detailed form of γ-ray yield curves will be presented. Greater accuracy was possible through the construction and use of a new electronic device which improved the methods of taking data.[14,15] The aluminum targets were prepared under conditions which minimized effects of contamination. Experimental results from the aluminum targets will be compared to calculated yield curves obtained by Monte Carlo techniques through the use of a newly formulated collision spectrum based on the Born approximation. Some studies on contamination effects of O_2 and N_2 gases on thick targets will also be presented.

II. EXPERIMENTAL

The stainless-steel target chamber is shown in Fig. 1 and has not been changed much from the form used by Costello *et al.*[6,7] It contains essentially five features: a target holder, a target evaporator, a titanium getter-ion vacuum pump,[16] an Orbitron ion gauge,[17] and a beam collimator. The Ta target holder is insulated from ground, but may be rotated in a threaded support so it moves vertically over a distance of 8 cm. It is driven by an external magnet and has four sides, each of which is capable of holding four targets, thus a maximum of 16 targets may be studied without vacuum interruption. The target backing is 0.05-mm Ta which is spot welded to the larger Ta target holder.

The target evaporator consists of a ball of aluminum held by a 1.5-mm Ta wire. During evaporation, the aluminum ball is at 3 kV and it is bombarded by electrons supplied by a 0.11-mm W filament. The power consumption is approximately 30 W. After evaporation of the target, the holder is turned 180° so the target is facing the incident beam.

Prior to evaporation of the target, the entire target chamber is baked at about 300°C for a period of 20 to 40 h. After the baking, the titanium pump is started and it reduces the pressure in the chamber to approximately 3×10^{-9} Torr.

For almost all of the targets prepared, the evaporations were performed at pressures usually 3×10^{-7} Torr or lower with fast evaporation rates. During the runs the pressure was usually about 3×10^{-9} Torr. These conditions were shown by Costello *et al.*[6,7] to be sufficient to avoid surface or volume contamination. For all of the yield data obtained under these circumstances, there was no evidence of contamination except when conditions were purposely arranged for their study.

Gamma radiation from the reaction was detected by NaI(Tl) crystals located on each side of the target chamber. The crystals were coupled to photomultiplier tubes which connected to separate amplifier and discriminator circuits.

To obtain the yield data as a function of proton energy the energy of the proton beam from the electrostatic generator was held constant while the voltage on the target was changed in a stair-step manner. The size of the step could be varied, but generally it was 100 V, with a time duration of about 0.5 sec per step. The number of steps (data points) could be varied between 8, 16, 32, or 64 steps. The yield for each step was sorted and stored in a Nuclear Data 256 channel analyzer (Model ND-101). The stair-step voltage was cycled many times for each yield curve obtained. This technique provided a uniform method for taking yield curves, it reduced problems due to changes in background, ion-source conditions, target conditions, beam current, and electronics. It was versatile as to the number and size of steps and eliminated the time lost in resetting the generator voltage when taking data point by point.

The electronic device which supplied the stair-step voltage to the target also had the additional function of correcting energy fluctuations in the beam. This energy modulating technique was based on an observation of

[14] J. G. Skofronick, M. F. Murray, and D. G. Costello (private communication).

[15] J. G. Skofronick, Ph.D. thesis, University of Wisconsin, 1964 (unpublished); available from Ann Arbor Microfilms Inc., Ann Arbor, Michigan.

[16] R. G. Herb, T. Pauly, R. D. Welton, and K. J. Fisher, Rev. Sci. Instr. **35**, 573 (1964).

[17] W. G. Mourad, T. Pauly, and R. G. Herb, Bull. Am. Phys. Soc. **8** (1963).

Parks *et al.*,[18,19] who found that the instantaneous beam from an electrostatic generator had a much smaller energy spread than the time averaged spread due to energy fluctuations in the beam. They found that the resolution of the beam from their electrostatic generator could be much improved by using a varying voltage on the target which corrected the beam energy fluctuations. An electrostatic analyzer was used to provide the error signal.

This energy modulation technique was combined with the stair-step voltage device and was used in obtaining all of the data to be presented.[14,15]

Because of a wedge-shaped gap between the plates of the one-meter electrostatic analyzer used in this experiment, resolutions in excess of 5000 could not be obtained. Thus a satisfactory check on the performance of the energy modulating part of this device was not possible. Work is now underway to correct this defect.

III. COMPUTATIONAL PROCEDURE

Palmer *et al.*[4] have shown that an expression for γ-ray yield for a resonance reaction located at E_R, for a target of thickness t and a mean beam energy E_B can be reduced to a form suitable for computer work. This expression is

$$Y(E_B,t)=\sum_i \mathcal{Y}_i \sum_{j=1}^{m} L_{ij}n_j, \tag{1}$$

where $n_j=1$ for a pure target and it gives the fraction of active nuclei in layer j of the target; the expression $\mathcal{Y}_i$ represents all the spreading factors and can be approximated by the yield data from a very thin target; the function L_{ij} is defined as the total track length for protons passing through the rectangle (i,j) and is obtained by Monte Carlo techniques; $t=m\Delta x$ where Δx is the thickness of each of the layers j; and i refers to energy index.

To obtain the total track length L_{ij}, a two-dimensional array is set up in the computer which consists of energy-distance rectangles. Protons are passed through this array where random numbers are used to select the distance traveled and energy lost between each collision. The particle path length in each rectangle (i,j) is recorded for each proton until a predetermined amount of energy has been lost at which time another proton is selected and the process is again repeated. If a sufficient number of protons are passed through the computer, then the L_{ij} can be obtained with good accuracy.

The distance X traveled between collisions is obtained from a random number R by:

$$X=-\lambda \log\left[\frac{R_{\max}-R}{R_{\max}-R_{\min}}\right], \tag{2}$$

[18] P. B. Parks, H. W. Newson, and R. M. Williamson, Rev. Sci. Instr. **29**, 834 (1958).

[19] P. B. Parks, P. M. Beard, E. G. Bilpuch, and H. W. Newson, Rev. Sci. Instr. **35**, 549 (1964).

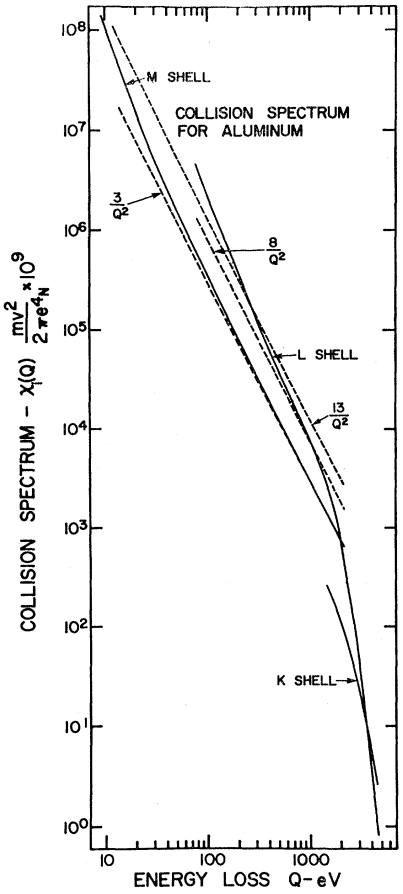

FIG. 2. Log-log plots of the free electron collision spectrum (dashed line) and the Bethe-Born collision spectrum (solid line).

where λ is the mean free path for collisions and is equal to the average energy lost per collision divided by the stopping power.

The energy lost, Q, in a collision is determined from a random number R by:

$$\int_{R_{\min}}^{R} dR=k\int_{Q_{\min}}^{Q}\chi(Q)dQ, \tag{3}$$

where $\chi(Q)$ is the collision spectrum: $R_{\min}$ and $Q_{\min}$ represent the lower limits for these variables; and k is a normalizing constant which is found by letting $R\rightarrow R_{\max}$ and $Q\rightarrow Q_{\max}$, which represent the upper limit of these variables.

The collision spectrum is defined such that $\chi(Q)dQdx$ is the probability that a proton traveling a distance dx in an absorber will suffer a collision in which the proton loses an energy between Q and $Q+dQ$. This $\chi(Q)$ does depend upon the incident proton energy E, as well as Q, but if the change in E is small, this dependence can be ignored. Since only a small energy range is considered (about 5 keV), this assumption is justified.

The collision spectrum is related to stopping power

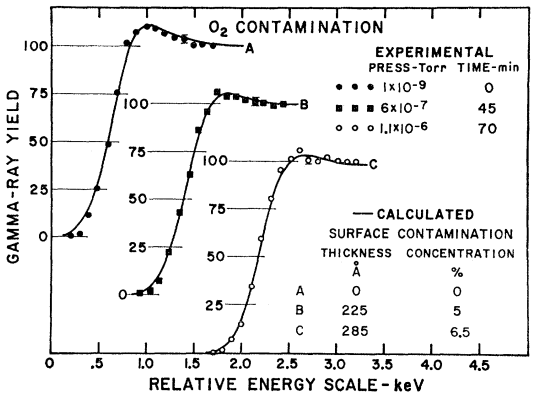

FIG. 3. Gamma-ray yield curves from aluminum showing effects of exposure to oxygen. Solid lines represent calculated curves. Contaminant could be lumps on the surface. Curve B would then be for lumps 225 Å thick covering 5% of the surface.

by:

$$\frac{dE}{dx}=\int_{\text{all}Q}\chi(Q)QdQ. \tag{4}$$

The result of Eq. (4) should agree with the nonrelativistic result[20] for stopping power:

$$dE/dx=(4\pi e^4/mv^2)NB, \tag{5}$$

where e is the charge and m is the mass of the electron; v is the velocity of the proton; N is the number of atoms per cm^3; and B is defined as the stopping number.[20] The stopping number can be written as:

$$B=Z\log(mv^2/I)-(\text{correction term}), \tag{6}$$

where Z is the number of electrons per atom and I, a constant equal to 163 eV for aluminum, is a mean ionization and excitation energy for the particular absorber and is obtained experimentally.

It is convenient to make the assumption that $B=B_K+B_L+B_M$; each shell of the atom contributes separately to the stopping number, and further to let $\chi(Q)=\chi_K(Q)+\chi_L(Q)+\chi_M(Q)$. With this notation the expression for stopping power for each shell can be written as follows:

$$\int_{\text{all}Q}\chi_i(Q)QdQ=\frac{4\pi e^4}{mv^2}NB_i \tag{7}$$

where $i=K$, L, or M.

The contributions to the collision spectrum by the K and L shells have been supplied by Merzbacher and Khandelwal[21] and are based on Bethe's treatment of stopping theory where the Born approximation is used.[12] Figure 2 shows the $\chi_i(Q)$ for both the K and L shells.

[20] H. A. Bethe and J. Ashkin, in *Experimental Nuclear Physics*, edited by E. Segre (John Wiley & Sons, Inc., New York, 1953), Vol. 1.

[21] E. Merzbacher and G. S. Khandelwal (private communications, 1963).

The L-shell contribution is compared with the Rutherford collision spectrum for free electrons which is indicated in the figure as a dashed line labeled $8/Q^2$.

The contribution to the collision spectrum from the M-shell electrons remains to be determined. Since the binding energies for the three electrons in this M shell are of the same magnitude as the binding in hydrogen, it is assumed that $\chi_M(Q)$, can be approximated by a form similar to that obtained by the Born approximation for 992-keV protons incident on hydrogen. This function was shown by Morsell[10,11] to be of the form:

$$\chi_i(Q)=\frac{2\pi e^4}{mv^2}NZ_i\left[\frac{1}{Q^2}+\frac{C_i}{Q^{3.28}}\right], \tag{8}$$

for $E_i\leq Q\leq 2160$ eV, and $\chi_i(Q)=0$ for all other Q. This is a good approximation to the spectrum for hydrogen if $Z_i=1$, $E_i=13.6$ eV, and $C_i=86.0$, where the subscript i labels the single electron of hydrogen.[10,11]

The parameters E_M and C_M for aluminum are obtained from energy-level tables and stopping-power theory, respectively. If it is assumed that the aluminum atoms are isolated, with no interactions between electrons in the M shell, then the energy to remove each of the three M-shell electrons can be obtained. These values are used to find a weighted minimum energy corresponding to E_M in Eq. (8). For the outermost electron ($3p$), the ionization energy is 5.98 eV.[22] The energy required to remove the $3s^2$ electrons is then 5.98 eV plus the energy required to excite the ion to a $3s\ 3p$ state. There are but two groups to consider: one group, a triplet, has a multiplicity of 9 and an energy of 4.65 eV while the other is a singlet with a multiplicity of 3 and an energy of 7.42 eV.[22] This gives 10.63 and 13.40 eV as the ionization energies of the $3s^2$ electrons. Using the multiplicities and the binding energies, a weighted minimum energy $E_M=9.1$ eV is obtained.

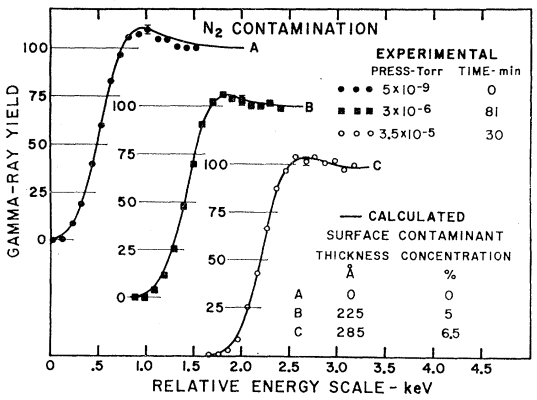

FIG. 4. Gamma-ray yield curves from thick aluminum targets showing effects of exposure to nitrogen. Lewis peak of curve A is slightly depressed because pressure during evaporation rose to 2.6×10^{-6} Torr.

[22] Natl. Bur. Std. (U.S.) Circ. 467.

If the stopping number for the atom is obtained from Eq. (6) and if the contributions from the K and L shell [Eq. (7)] are subtracted from this stopping number, then the stopping number for the M shell can be obtained. If Eq. (7) is again used with this stopping number then C_M of Eq. (8) is found to be 45.4. With C_M and E_M determined, Eq. (8) is completely specified for the M shell of aluminum, and it is shown in Fig. 2 where it is compared to a collision spectrum for three free electrons which is labeled $3/Q^2$. Also shown is a collision spectrum labeled $13/Q^2$ which is that obtained if all the electrons of the atom are treated as if free. This was the spectrum used by Walters *et al.*[2,3] and Palmer *et al.*[4]

IV. THICK-TARGET RESULTS—CONTAMINATION EFFECTS

The experimental data in curve A of Fig. 3 was obtained from a freshly evaporated aluminum target, while curves B and C were taken on the same target while O_2 was bled into the vacuum system at pressures of 6×10^{-7} Torr and 1.1×10^{-6} Torr, respectively. The Lewis peak appears to be reduced by the O_2. Similar results are shown in Fig. 4 for N_2.

The solid curves in these two figures are calculated by the method previously described. Consider the solid line in curve A, Fig. 3. It is obtained by Eq. (1) where the function L_{ij} is generated with Monte Carlo techniques by passing 15 000 protons through the computer, while the function Y_i is approximated by the yield data from a very thin target. The solid points of Fig. 5 show the yield data taken under experimental conditions similar to that for the data presented in this paper. The solid points show some asymmetry due to straggling and nonuniformities in the target. The experimental data are made symmetric by reflecting the low-energy data about the peak to the high-energy side and these points are shown as open circles. The solid curve is a Gaussian function fitted to the experimental data which is used to approximate Y_i and this represents all of the effects on the yield due to beam spread, Doppler broadening

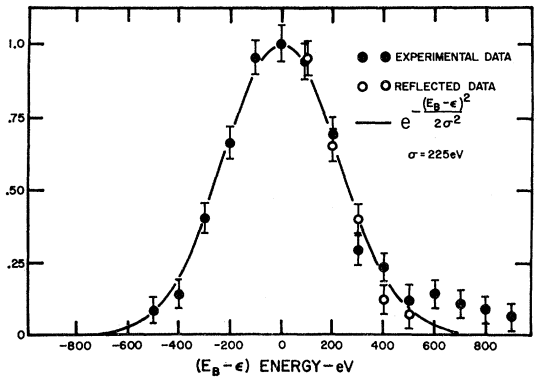

FIG. 5. Gaussian curve fitted to gamma-ray yields from thin target of aluminum. This is used to approximate the function Y_i of Eq. (1).

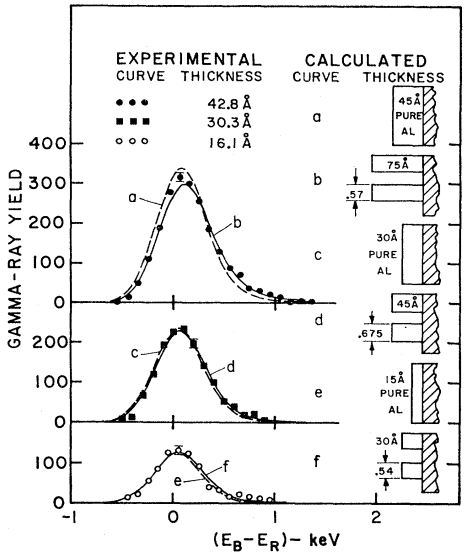

FIG. 6. Comparison of experimental yield data from semithick aluminum targets with calculated yield curves obtained by using the Bethe-Born collision spectrum. A noncontinuous target gives best calculated fit (solid line) to the data. Mean beam energy E_B is plotted relative to resonance energy E_R.

and resonance width. With these expressions for L_{ij} and Y_i, the summation of Eq. (1) gives the calculated thick-target yield curve shown as curve A in Fig. 3. Curve B of Fig. 3 is calculated by assuming a 5% inactive contaminant with stopping power equal to that of aluminum, which extends into the target to a depth of 225 Å. Curve C of Fig. 3 is calculated by assuming there is a 6.5% inactive contaminant which extends into the target to a depth of 285 Å. The calculated curves of Fig. 4 are obtained in a similar manner.

The results of these figures show that exposure of fresh aluminum targets to either O_2 or N_2 gas reduces the Lewis peak by surface contamination and it appears that N_2 contaminant effects take place more slowly than O_2 contaminant effects. In contrast Costello *et al.*[6,7] found that CO and CH_4 had no such effect.

V. SEMITHICK TARGET RESULTS

The procedure followed in obtaining the experimental data from semithick targets was as follows: the electronic device previously described was used to obtain the yield from a thick target; then a semithick target was evaporated and yield data from it were taken. Comparison of the two sets of data then established the relative energy scale between the curves.

Since the electronic device had no provisions for integrating the proton beam, a number of data points were taken for each semithick target in the region of the peak with the older technique of changing the mean energy of the beam through the electrostatic analyzer and integrating the beam current for each point. This was followed with the same integration techniques on

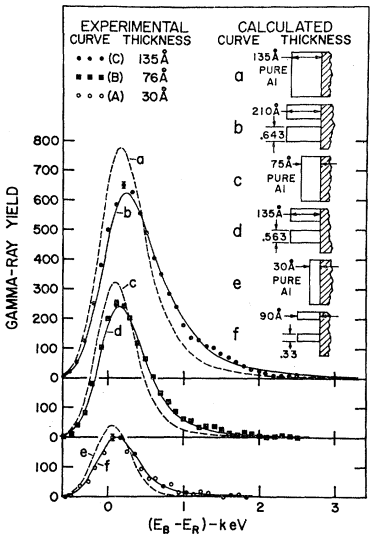

FIG. 7. Comparison of experimental yield data from semithick aluminum targets with calculated yield curves. Best calculated fits (solid lines) are obtained by assuming targets are uniform islands (noncontinuous target) with fraction of target backing not covered by aluminum.

the plateau of a thick target. The thick-target data were normalized and the integrated points were used to adjust the relative height of the semithick target yields to the same normalization as the thick target. This comparison of semithick and thick-target data was then used to determine the thickness of the semithick targets according to a relation shown by Palmer *et al.*[4] to be

$$t=\frac{\text{area under semithick-target curve}}{\text{height of plateau of thick-target curve}}.$$

The calculated curves are such that each has an area equal to the area enclosed by the experimental data points, except in the comparison of the calculated yield for a pure (uniform) target, where sometimes the area is slightly larger or smaller than that enclosed by the experimental data.

This was a result of the storage capacity of the computer which limited the thickness of the calculated curves to multiples of 15 Å. The configurations of the calculated curves are shown schematically on the figures.

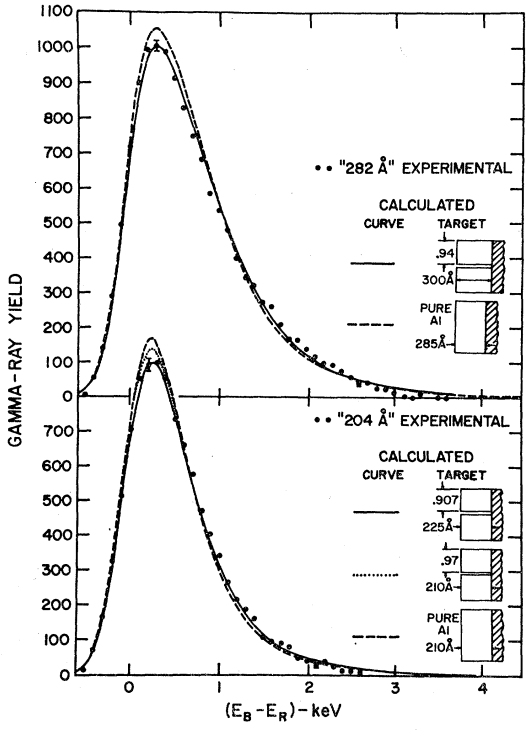

FIG. 8. Comparison of experimental yield data from semithick aluminum targets with calculated yield curves. Best calculated fits are obtained by assuming much smaller gaps between islands than those used in Figs. 6 and 7.

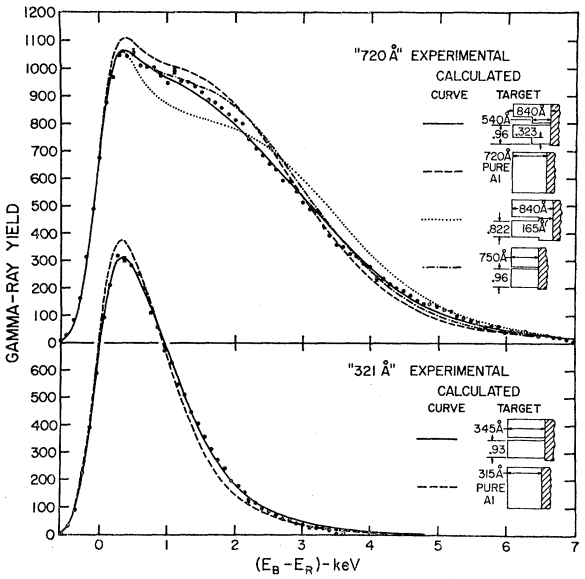

FIG. 9. Comparison of experimental yield data from semithick aluminum targets with calculated yield curves. Data from 720 Å target has for its best calculated fit the yield from a discontinuous, nonuniform target. Yield curves from targets of this thickness are likely to be the most sensitive to target nonuniformities.

Figures 6 and 7 show the data points for targets less than 200 Å thick. To obtain good calculated fits to these data, the targets are assumed to be made of islands of uniform thickness with a large fraction of the target backing not covered by aluminum. All of these data are fitted relatively well by this simple assumption of noncontinuous targets and in each case the best calculated fit is shown as a solid line.

The form of nonuniformity chosen is probably not unique but this assumption appears reasonable in light of the work of Sennett and Scott[23] who found that very thin evaporated films usually consisted of islands which become continuous as the films become thicker. Their

[23] R. S. Sennett and G. D. Scott, J. Opt. Soc. Am. **40**, 203 (1950).

evidence further showed that the thickness at which the films became continuous and relatively uniform depended on the metal being evaporated, the evaporation rate, the target backing temperature and the material of the backing.

Figures 8 and 9 show yield results from targets thicker than 200 Å. Good calculated fits are obtained with much smaller gaps between the islands which seems to bear out the observations of Sennett and Scott.[23] Note that the 720 Å yield data in Fig. 9 has for its best calculated fit the yield from a discontinuous, nonuniform target. This seems to indicate that the islands of this target were growing both vertically and horizontally, but had not yet combined to form a continuous film.[24]

Figure 10 shows some of the data of Figs. 6 to 9 replotted as a family. It also includes thick-target data. The solid lines represent the previous best fits to the experimental data. The experimental data of the 720 Å target does not join that for a thick target in the region of the Lewis peak and the beginning plateau, whereas the calculated curves for uniform targets in Fig. 11 predict that they should join together. This has been observed before in the experimental work of Palmer *et al.*,[4] but no explanation for it was advanced. The probable cause now seems to be nonuniform films. It is very likely that yield curves for targets of this thickness may be particularly sensitive to target nonuniformities.

Calculated yield curves obtained by using the $1/Q^2$ spectrum (dashed lines) and the B-B spectrum (solid lines) are shown in Fig. 11. A close examination of the pairs indicate significant differences for both the semithick and the thick-target yield curves. The calculated semithick-target yield curves from the B-B spectrum, as compared to those from the $1/Q^2$ spectrum, rise more slowly on the low-energy side, have a lower peak which is shifted toward higher energy, and have a trailing edge

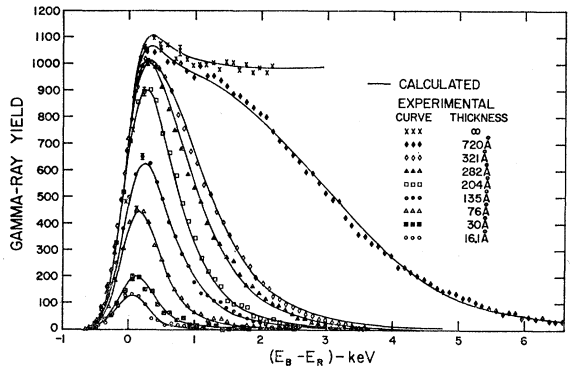

FIG. 10. Some of the experimental data and best fit calculated curves of Figs. 6 to 9 replotted as a family. Energy scale is that predicted by the calculated curves, but in all cases the differences between calculated and experimental predictions were less than 50 eV.

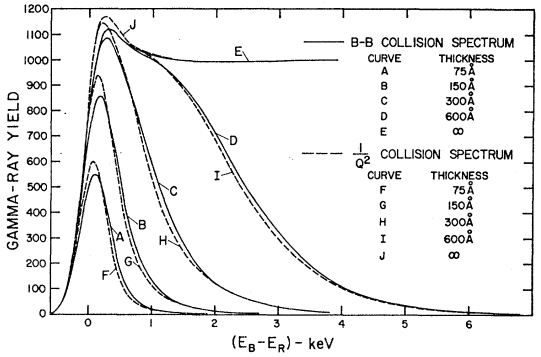

FIG. 11. Comparison of calculated yield curves obtained from the $1/Q^2$ collision spectrum to those from the Bethe-Born collision spectrum.

that drops off more slowly than that obtained from the $1/Q^2$ spectrum.

In comparing the calculated thick-target yield curves from the two spectra of Fig. 11, the results from the B-B spectrum predict a Lewis peak which is lower and shifted toward higher energy than that predicted by the $1/Q^2$ spectrum. Experimental thick-target data are easily fitted with the results from the B-B spectrum as is shown in Fig. 3. The reason for the better fit has already been shown by Costello *et al.*[6,7] to be a result of accounting for the resonance contributions to the collision spectrum. No comparison is made with yield curves from the C-S spectrum because only curves for thick targets are available and these have been shown by Costello *et al.* to fit the experimental data.

VI. CONCLUSION

The detailed form of yield curves from semithick targets appears to have been experimentally determined in this work much more closely than in any previous results. Contamination effects appear to have been eliminated and only some nonuniformity effects remain. Also in calculations of these curves, substantial improvement is believed to have been realized with major uncertainties remaining in the collision spectrum only in the low-energy loss region.

One purpose of this work was to establish more closely target conditions that must be met to give reproducible yield curves characterized only by fundamental factors such as nuclear resonance width, Doppler broadening, and the collision spectrum, rather than features such as the thickness of cracked pump oil films covering the target. Progress toward this goal has been made.

Results of this work show that both O_2 and N_2 can cause surface contamination. Studies on residual gases in vacuum systems[25] show that the amount of these gases present is small and so they probably are not responsible for contamination as observed by Walters

[24] K. H. Behrndt, Vacuum **13**, 337 (1963).

[25] T. Pauly (private communications, 1964).

et al.[2,3] and Costello *et al.*[6,7] Since it is known that water vapor and the heavier hydrocarbons are present in vacuum systems,[25] further experimental work with these gases is needed.

Results show that variations in target thickness remains as a problem and that improvement in target preparation methods is needed.

Work is now in progress toward improvement of the resolution of the electrostatic analyzer used for this work. With better resolution, further progress is expected toward reducing the uncertainties remaining in regard to the factors which determine the form of resonance yield curves.

Reproducibility of energy standards and intercomparison of these standards between laboratories will then be more straightforward and determination of nuclear resonance widths from yield curve shapes may be more commonly realized.

ACKNOWLEDGMENTS

The authors are indebted to Professor M. B. Webb, C. H. Blanchard, K. R. Symon, and H. W. Lewis for many helpful discussions. In particular the authors are indebted to Professor E. Merzbacher for his help with the collision spectrum. The expert aid of M. F. Murray in his design of the electronics used in this work is appreciated. The authors also wish to thank R. J. Nickles, K. E. Nielsen, and R. A. Due who assisted in taking the data.

PHYSICAL REVIEW VOLUME 135, NUMBER 5A 31 AUGUST 1964

Proton Energy-Loss Distributions from Thin Carbon Films*

A. L. MORSELL†
University of Wisconsin, Madison, Wisconsin
(Received 17 January 1964; revised manuscript received 1 May 1964)

A 992-keV proton beam, limited in energy spread by a 1-m electrostatic analyzer, passes through a thin carbon film before entering a second 1-m electrostatic analyzer. The energy distribution of protons in the second analyzer is measured by sorting proton counts from a detector at the analyzer exit according to the instantaneous value of a sweep voltage applied to one of the analyzer plates. A combined resolution of 30 000 was obtained for the double-analyzer system. Carbon films with thicknesses corresponding to mean energy losses ranging from several keV down to about 200 eV have been studied. Several of the experimental energy-loss distributions are compared with distributions computed by Monte Carlo techniques for three different assumed discrete energy-loss spectra. Good fits are obtained from a new spectrum constructed using the results of some computations by E. Merzbacher.

INTRODUCTION

THE statistical process by which high-energy charged particles lose energy as they interact with the atomic electrons of a target material may be completely described by what will be called the discrete energy-loss spectrum, a function which gives the probabilities for energy-loss jumps of varying magnitudes. This function is needed for proper handling of the energy-loss process in many experimental situations; knowledge of the stopping power of the target material or of the range of the high-energy particles in the material is often not sufficient. Unfortunately, the discrete energy-loss spectra are not available in the literature in any convenient form, and there has been virtually no experimental effort directed toward determining them.

The present work represents an attempt to obtain measurements which will provide information about these fundamental functions. A nearly monoenergetic beam of protons is allowed to pass through a thin carbon film, and the resultant energy-loss distribution of the protons is measured. If the target film is thin enough and the resolution high enough, the energy-loss distribution should be a moderately sensitive function of the discrete energy-loss spectrum of the material. An attempt is made to construct a close approximation to the true discrete energy-loss spectrum for use in computing energy-loss distributions to be compared with the experimental results.

DESCRIPTION OF THE EXPERIMENT

The physical layout of the experiment is schematically shown in Fig. 1. The proton beam from the 3-MeV Wisconsin Electrostatic Accelerator, after passing through a magnetic analyzer and a pair of electrostatic quadrupole lenses, traverses a cylindrical electrostatic analyzer, which selects only those protons with energies close to a mean energy determined by the potentials on the cylindrical plates. The protons then pass through a target film and traverse a second electrostatic analyzer. Protons selected by this analyzer are scattered by

* Work supported in part by the U. S. Atomic Energy Commission.
† Present address: High Voltage Engineering Corporation, Burlington, Massachusetts.